WELDING RESEARCH

SUPPLEMENT TO THE WELDING JOURNAL, MAY 1978

Sponsored by the American Welding Society and the Welding Research Council

Electron Beam Welding Cavity Temperature Distributions in Pure Metals and Alloys

The presence of volatile constituents leads to peak temperature differences as much as 650 C between aluminum alloys and 470 C between three steels

BY D. A. SCHAUER, W. H. GIEDT AND S. M. SHINTAKU

ABSTRACT. The adaption of a narrow band infrared radiation pyrometer for measurements of the surface temperature variation in an electron beam welding cavity is described. Results are presented for welds in 1100, 2024, 5083 and 6061 aluminum as well as Type 304 stainless steel together with 20-6-9 and HY-180 steel, and tantalum.

Average peak temperatures for aluminum decreased from a maximum of 1900 C (3452 F) for the 1100 aluminum alloy to 1250 C (2282 F) for the 5083 alloy and 1080 C (1976 F) for the 7075 alloy. For the Type 304 stainless and 20-6-9 and HY-130 steels, peak values were 2100, 1820 and 2290 C (3812, 3308 and 4154 F) respectively.

This change was shown to be due to the presence of relatively volatile constituents in the alloys. It was also found that for a specific material the peak temperature did not vary significantly with penetration depth.

Introduction

The current interpretation of the electron beam welding process is that as the kinetic energy of the electron beam (EB) is absorbed by the workpiece, melting and vaporization of the metal occurs. Due to the reaction effect of the vaporizing atoms a cavity is formed. During quasi-steady operation it is postulated that the EB passes through the metal vapor in the cavity and is absorbed at the base and walls. The resulting vapor pressure force on the base and the wall of the cavity is balanced by the hydrostatic pressure and surface tension forces of the molten metal lining the cavity.

Based on the above interpretation a quasi-equilibrium force balance in an EB cavity indicates a required base temperature of approximately 1900 C (3452 F) for welds in pure aluminum[1] and 2400 C (4352 F) for iron. At these temperature levels there is a strong variation of vapor pressure with temperature, and it was therefore postulated that relatively small changes in cavity surface temperature could be very important in the stability of an EB weld cavity. Furthermore, it was suggested that small amounts of relatively volatile alloying elements would have a substantial effect on vapor pressure, and consequently should influence cavity surface temperatures and welding stability.

The potentially fundamental and practical importance of EB welding cavity surface temperatures as described above prompted consideration of the experimental study presented herein. In order to obtain local temperatures a small target infrared detector* was adapted for observations inside the cavity. The system developed is described in the following section. This is followed by results obtained for aluminum and several of its alloys, three steel alloys and tantalum.

Experimental Program

Welding cavity temperature measurements were made in two different EB welding machines. Both were low voltage-high amperage units. The temperature measuring system developed

Information presented in part at the AWS 59th Annual Meeting held in New Orleans, Louisiana, during April 3-7, 1978.

D. A. SCHAUER is with the Nuclear Explosives Division, Mechanical Engineering Department, Livermore Laboratory, University of California, Livermore, California; W. H. GIEDT is Associate Dean—Graduate Study, College of Engineering, University of California, Davis, California; and S. M. SHINTAKU is with the Getty Oil Company, Taft, California.

**Vanzetti Infrared and Computing-Systems Model 1262.*

for the first† (which will be referred to as the SBI) is shown in Fig. 1. To clear the focusing coil the viewing angle of the probe relative to the workpiece surface has to be approximately 45 deg. Radiation from a small target area (~0.5 mm at 0.02 in. in diameter) passed through a small aperture in a protective housing. It was then reflected by a mirror onto the end of the optical sensing probe. The radiation is focused by a lens system on the end of a fiber optical cable as shown in Fig. 1. The focal length of this system was 13 in. (0.33 m). The radiation is then transmitted through the cable to a lead sulfide detector cell where it is converted into an electrical signal.

During welding the vapor from the molten metal will deposit on any surface in direct sight of the cavity. To prevent deposition on the focusing lens of the measurement probe a mirror was inserted in the optical path. Tests revealed that the mirror reflectivity changed during the first 3-6 seconds (s) after the start of welding. After this initial change the vapor continually plated onto the mirror over the duration of the experimental measurement but does not change the reflectivity of the mirror appreciably for the next 60-100 s. Therefore, continuous temperature measurements could be obtained during welding.

The lead sulfide detector cell of the optical probe system has a radiation wavelength response band of approximately 1 to 2.5 micrometers. The manufacturer recommends treating instrument measurements as monochromatic at an effective wavelength of 1.4 micrometers. Variation of this effective wavelength with temperature is indicated to be negligible. The signal from the detector is amplified and displayed as a direct current potential on an electronic digital console. The full scale response time is approximately 2.5 milliseconds. The DC output potential was recorded on a strip chart recorder. The radiant temperature or brightness temperature was then determined from calibration data. If the spectral emittance of the specimen is known, the surface temperature can then be calculated. (The effect of absorption and emission of radiation by the metal vapor in a welding cavity was estimated to be negligible.)

The infrared radiation pyrometer was calibrated with two blackbody cavities, one operating up to a temperature of 1000 C (1832 F) and the other operating in a temperature range of 1100 to 3000 C (2012 to 5432 F). The accuracy of the calibration equipment was approximately ±1%. The radiation pyrometer has a temperature resolution of 2%. Therefore, the accuracy of the obtained calibration data is considered to be approximately ±3%.

In the second welding machine†† (referred to as the BTI) used, the electron gun configuration permitted location of the optical sensing probe so as to sight almost directly down in the welding cavity. As indicated in Fig. 2, the installation included a device for moving a teflon film across the optical probe opening at a rate of 1.8 cm/s to protect it from metal vapor deposition. Attenuation of the radiation by this film was found to be approximately 5% and was accounted for in the calibration of the optical probe. A mechanism for moving the probe back and forth across the cavity was also incorporated. The response of the amplifying and readout unit used with this welding unit was about 100 ms compared to 2.5 ms for the unit used with the SBI. As a result, rapid temperature excursions were not observed.

Experimental Procedure

In the SBI the metal to be welded was rotated around an axis underneath the EB resulting in a circular weld bead. Temperature measurements were obtained while welding the following materials: aluminum and aluminim alloys—1100, 6061, 5083, and 7075; steel alloys—20-6-9, HY-180 and Type 304 stainless steel; and finally pure tantalum.

The particular alloys chosen contained small but significant amounts of volatile species. To facilitate comparison of the behavior of the aluminum materials pie shaped sections were cut and then mounted to form a complete circular plate. A detailed description of the test equipment and procedure is given in the literature.[2] During welding the same machine settings were used for each complete revolution of the plate. All of the other materials were welded separately.

Welding runs were performed at various weld speeds over the range of 10 to 60 ipm (4.2 to 25.4 mm/s), and power setting ranges of 13 to 20 kV and 100 to 270 milliamps (mA). Temperature profiles perpendicular and parallel to the weld were obtained for several of the materials.

Voltage and current parameters selected for many of the test welds resulted in a shallow weld cavities. This allowed the probe to be sighted on or near the cavity bottom even with a 45 deg viewing angle. For a typical weld sequence the beam was turned on and the position of the temperature measuring spot was manually positioned by controls outside the electron beam chamber. To obtain the cavity temperature at the cavity bottom, the controls were adjusted during welding to obtain peak output on the strip chart recorder. This was assumed to be the cavity temperature at the bottom. Once the maximum reading was obtained, the probe was not moved for the duration of this particular test weld. This allows continuous recording and observation of the temperature history in the region that represents the cavity bottom.

In the BTI the workpiece is moved linearly under the EB. Cavity temperature measurements were made on Type 304 stainless steel, Al-1100, Al-2024 and Al-6061. The beam potential was set at 31 ± 2 kV for all runs. The beam current was 155 ± 5 mA for stainless steel and 135 ± 5 mA for aluminum and its alloys. Temperature profiles parallel and perpendicular to the weld were measured at speeds of 0.5, 0.8, and 1.2 cm/s for each material. Special effort was made to locate the sensing probe so that it would pass over the bottom of the cavity. Unfortunately, due to the small cavity dimensions, and possible small variation in cavity location with time, it is possible that the peak output of the probe did not correspond to sighting of the cavity bottom. Additional details about the experiment apparatus may be found in the literature.[3]

Interpretation of Measurements

The infrared radiation probes used in this study measure the rate of radiant energy emitted from a molten metal surface in a small solid angle subtended by the focusing lens—Figs. 1 and 2. Assuming the intensity of radiation from the molten metal surfaces viewed was uniform with probe sighting angle (i.e., the Lambert cosine law was satisfied), the spectral intensity is expressed in terms of the spectral emittance by:

$$i_\lambda = \frac{e_\lambda(T_s)}{\pi} = \frac{e_{\lambda b}(T_r)}{\pi} \qquad (1)$$

where $e_\lambda(T_s)$ is the hemispherical emissive power of a typical specimen surface at T_s and $e_{\lambda b}(T_r)$ the emissive power of a blackbody at an effective (radiant) temperature T_r. In terms of the hemispherical spectral emittance of the specimen surface ϵ_λ, $e_\lambda(T_s) = \epsilon_\lambda e_{\lambda b}(T_s)$. Introducing the Planck law for $e_{\lambda b}(T_s)$ and $e_{\lambda b}(T_r)$ (and deleting the −1 terms in the denominators) yields the following results for T_s:

$$T_s = \left[\frac{\lambda_e}{C_2} \ln \epsilon_\lambda + \frac{1}{T_r} \right]^{-1} \qquad (2)$$

†*Sciaky Brothers, Inc., Model No. VX rated at 32 kV and 500 mA.*

††*Brad Thompson Industries; rated at 50 kV and 200 mA.*

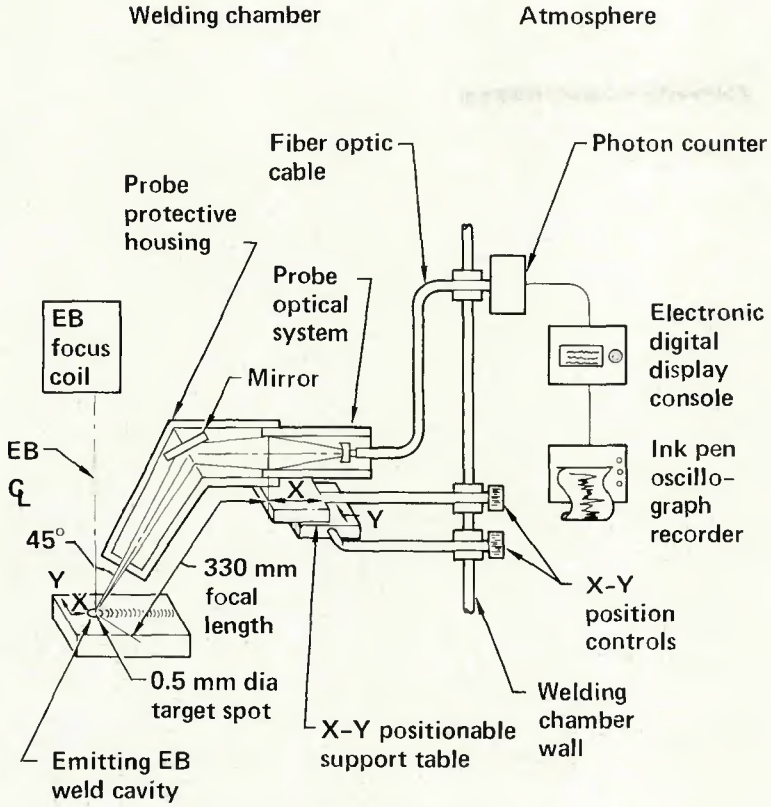

Fig. 1—Schematic of temperature measuring system

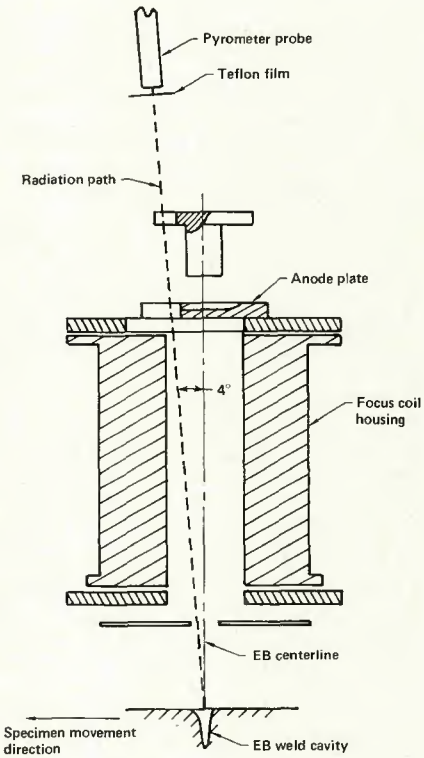

Fig. 2—Radiation path from EB weld cavity to probe

Here λ_e is the effective wavelength of the pyrometer, C_2 is the second Planck constant = 1.4387 μm°k, T_r the apparent (radiant) blackbody temperature indicated by the probe, and ϵ_λ the spectral emittance of the surface.

Application of this relation requires a value for ϵ_λ. Unfortunately no data could be found for this property for molten metals at wavelengths around 1.4 μm. A value for a particular material was determined by sighting the radiation probe on a molten metal pool of a material being welded and recording the output as the pool solidified. Using the known melting temperature and the value of T_r corresponding to the solidification plateau of the cooling curve a value of ϵ_λ would be calculated from equation (2).

In the SBI it was also necessary to measure the reflectivity ρ_λ of the mirror used in the optical system since the intensity of radiation reaching the probe would be $i_{\lambda p} = \rho_\lambda i_\lambda$. With this measurement included values of ϵ_λ obtained are listed in Table 1.

Theory indicates that the total spectral emissivity of metals increases linearly with temperature.[4,5,6] Experimentally measured total emissivity values of metals over extended temperature ranges tend to verify the theory.[7] However, as temperature increases, the spectral emissivity decreases for wavelengths below 1 μm and increases for wavelengths above 2 μm.[6] The effective wavelength (1.4 μm) of the pyrometer used is in this transition region. Since the temperature dependence of the spectral emissivity was unknown over the entire experimentally measured temperature range, a constant value was used.

Cavity Effect on Temperature Measurements

Another problem in measuring temperatures of the molten metal in a cavity is that since the cavity is deep and narrow, radiation from the inner surface will include both emitted and reflected components. This effect can be accounted for by using the following equation:

$$T_s = \left[\frac{\lambda_e}{C_2} \ln \epsilon_{\lambda a} + \frac{1}{T_r} \right]^{-1} \qquad (3)$$

where $\epsilon_{\lambda a}$ is an apparent spectral emittance.

A solution for the radiant interchange between the inner surface elements of a conical cavity with a uniform surface temperature by Lin and Sparrow[8] allows an estimate to be made for the cavity effect. The apparent spectral emittance for use in equation (3) is approximated to be:

$$\epsilon_{\lambda a} = \epsilon_\lambda + (1 - \epsilon_\lambda)\epsilon_\lambda E_{dA_i - A_s} \qquad (4)$$

where ϵ_λ is the spectral emittance of the cavity surface and $E_{dA_i - A_s}$ is the exchange factor. The increase in $\epsilon_{\lambda a}$ for temperature measurements made in shallow cavities can range from 10% at the top to 40% at the bottom. The accuracy of these values are dependent on factors which are not precisely known (such as partial specular diffuse reflection, variation in the cavity geometry as a function of time and variation in the surface spectral emittance). Fortunately, however, a highly precise value of $\epsilon_{\lambda a}$ is not needed to obtain a good approximation to the surface temperature.

Table 1—Emittance Values of Liquid Metals Measured at Melting Temperatures and at an Effective Wavelength of 1.4 Microns

Material	Emittance
Aluminum	0.20
304 stainless steel	0.36[a]
20-6-9 steel	0.42
HY-180 steel	0.26
Tantalum	0.28

[a] Tests in the BTI welding unit yielded an average value of 0.37.

Results

Electron Beam Welding Cavity Temperature Distributions

To obtain the temperature distribution in a weld cavity produced in the SBI, the location in the cavity on which the pyrometer was focused was changed during a test weld. This resulted in records such as is shown in Fig. 3. Note that the temperature fluctuations with time increase as the centerline is approached. However,

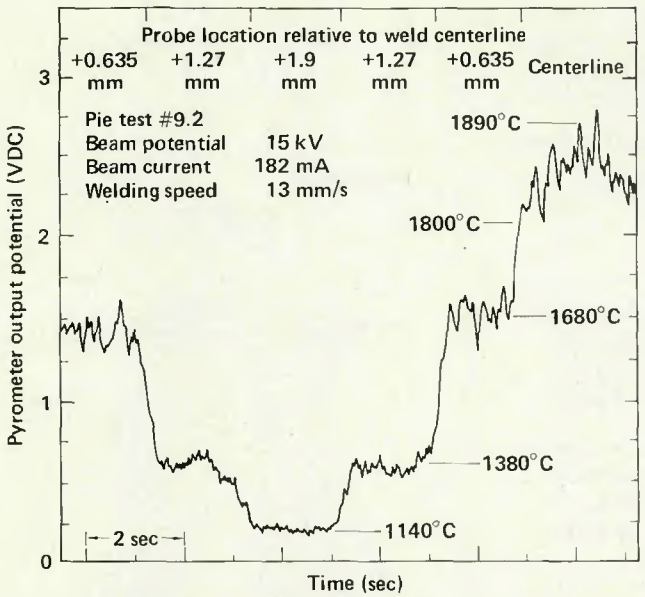

Fig. 3—Oscillograph record of a typical temperature history of an aluminum 6061 EB weld cavity as the pyrometer measurement location was varied perpendicular to the weld direction

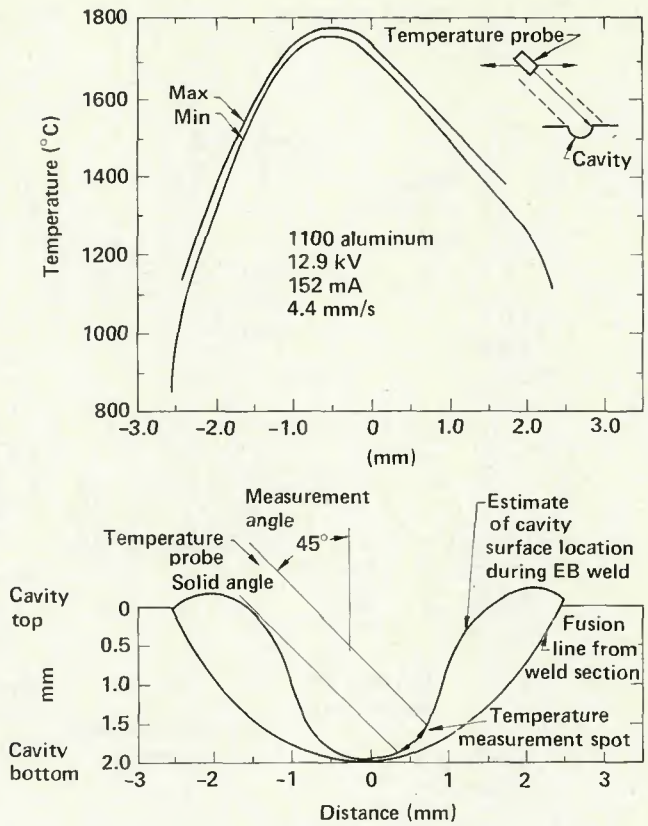

Fig. 4—Measured temperatures across 1100 Al weld cavity during one pass EB weld and approximated cavity shape based on weld section. Also shown is the geometrical relationship between the temperature probe and the liquid material surface

the maximum excursions are only on the order of 100 C (180 F) so that a mean value can be easily defined. Temperatures from a series of local measurements yielded distributions as illustrated in Fig. 4, for Al-1100. The curve labeled "max" is for the upper envelope of the probe response record, and that labeled "min" is for the lower envelope.

Similar results obtained with the BTI are shown in Fig. 5. Temperature distributions were evaluated from the measured pyrometer response using values of $\epsilon_{\lambda a} = 0.2$ and 0.5. The first value would apply if no cavity interreflections were present. The second $\epsilon_{\lambda a} = 0.5$ was estimated to apply to a conical cavity of approximately 15 deg half angle. Since $\epsilon_{\lambda a}$ would be expected to vary from 0.5 near the base to 0.2 at the cavity opening, the true temperature distribution varies from $\epsilon_{\lambda a} = 0.2$ curve at the opening to $\epsilon_{\lambda a} = 0.5$ curve along the cavity sides.

In view of the narrowness of the cavity in the base region and the fact that molten fluid was flowing in and out, there is some question as to whether the maximum base temperature was observed with the probe in these tests. Because of this it is believed that the temperature at the base shown for $\epsilon_{\lambda a} = 0.5$ is low and that the actual value falls between the peak values for the two curves shown. Note that the average value is about 1900 C (3452 F) which is in good agreement with the results from the SBI.

The temperature measurements were obtained for many different machine power settings and welding speeds but the observed peak temperature remained relatively constant for a specific material. Weld sections revealed that spiking occurred during several of the test welds. Detailed analysis along the centerline weld section of these welds exhibiting spiking did not show any correlation with the measured temperature levels corresponding to the region containing spiking.

Effect of Alloying Elements

To demonstrate the effect of volatile elements in an alloy on the cavity temperature and to make a direct comparison of several alloys the following test set-up was devised. Four 90 deg pie-shaped flat plate specimens of aluminum alloys 1100, 5083, 6061, and 7075 were fabricated and assembled to form a circular plate as shown in Fig. 6. During a test sequence, the machine power setting (SBI) and welding speed were maintained constant for a weld pass through all four materials. Peak temperature measurements, using the method previously described, indicated that the cavity temperature was highest for the 1100 aluminum and lowest for the 5083 and 7075 aluminum alloys.

As the magnesium and zinc contents of the aluminum alloys (1% Mg), 5083 (4.5% Mg) and 7075 (2.5% Mg, 5.5% Zn) increase, the peak measured temperature decreases. Essentially the same vapor pressure is required to maintain equilibrium in each of these welds. Since the elemental vapor pressures of these volatile elements are orders of magnitude greater than pure aluminum, the presence of a small fraction of them results in sufficient vapor pressure to produce a cavity at a lower temperature than for pure aluminum. The substantial effect of these alloying elements is illustrated in Fig. 7, which shows a pyrometer record of a test weld in 1100 aluminum with a small 7075 aluminum alloy sample placed in the weld path. Values of the peak temperatures measured for these alloys and other metals are listed in Table 2.

Cavity temperature distribution in alloys is illustrated in Figs. 8 and 9 for Al 7075 and 20-6-9 steel. Note that the temperature tends to decrease slowly near the bottom (center) of the cavity but rapidly near the top. This can be attributed to the higher beam energy flux near the center and to less constriction of the vapor near the cavity opening.

Material Composition Change of Alloy in Weld Region

A weld test series on the aluminum alloys 1100, 5083, 6061, and 7075, in which repetitive weld passes (with the SBI) were made over the same weld

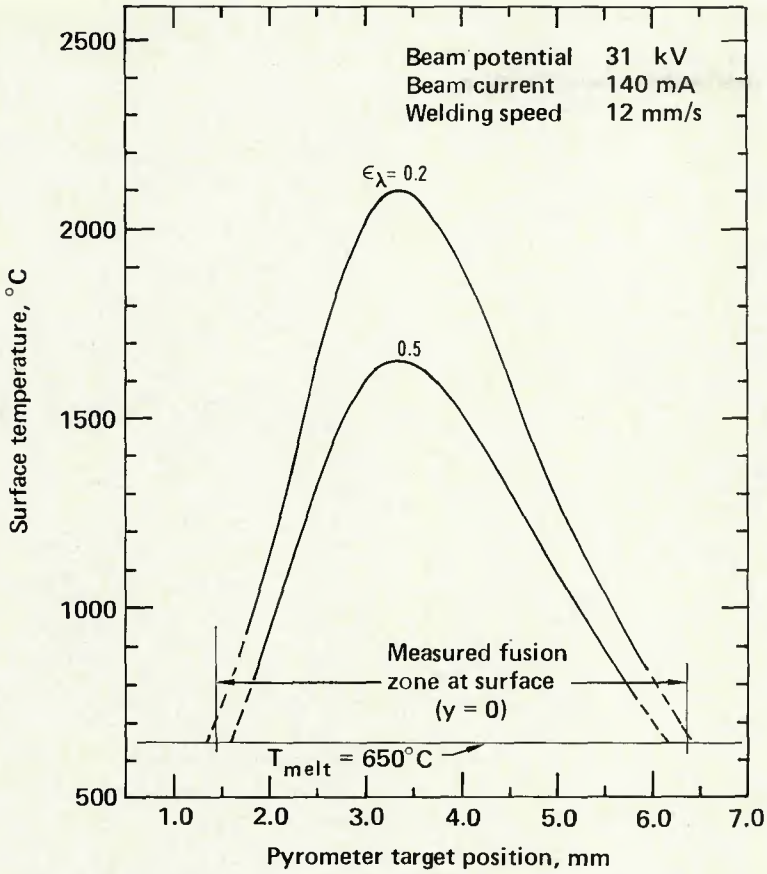

Fig. 5—Typical aluminum EB welding cavity temperature distribution perpendicular to weld

bead region yielded changes in observed peak temperatures shown in Fig. 10. The increases in measured peak temperatures with an increase in number of weld passes were found to be associated with a depletion of highly volatile elements in the weld bead region.

A microanalysis of each weld section after 6 weld passes revealed decreases in the amounts of the most volatile element as shown in Table 4. A chemical composition analysis of a deep penetration weld (115 mm) in a steel alloy produced similar results,[9] in that only the concentration of the most volatile element, manganese, was reduced for a single pass EB weld from 0.87 to 0.17%. This test series on the aluminum alloys suggests that a very small reduction in concentration of the volatile elements results in a significant and easily detectable change in the peak cavity temperature.

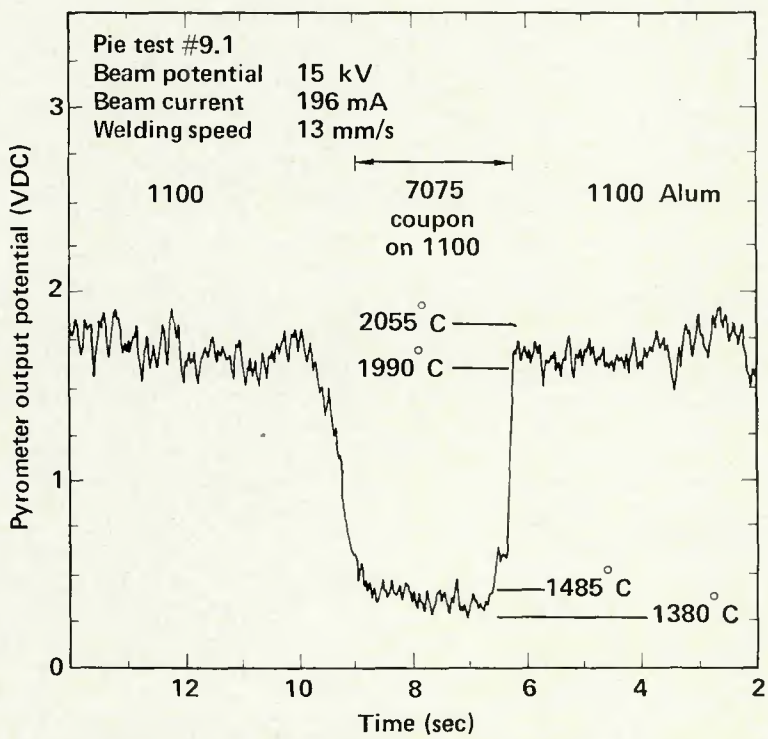

Fig. 7—Oscillograph record of a typical temperature history of an aluminum 1100 EB weld cavity base with a 1.8 mm thick aluminum 7075 sample inserted in weld path on top of aluminum 1100

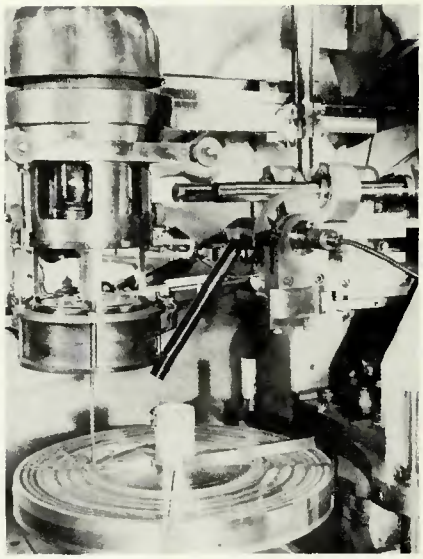

Fig. 6—Focused probe optical system and protective housing mounted on x-y positionable support table in welding chamber

Prediction of Peak Temperatures

The validity of the measured temperatures was tested by comparison with weld cavity base temperatures predicted assuming that the metal

Table 2—Representative Peak Temperatures

Material	Temperature, °C	Temperature variation, °C
1100 Al	1900	± 100
2024 Al	1700	± 100
5083 Al	1250	± 100
6061 Al	1800	± 100
7075 Al	1080	± 100
Type 304 stainless steel	2100	± 50
20-6-9 steel	1820	± 40
Hy-180 steel	2290	± 60
Tantalum	4440	± 150

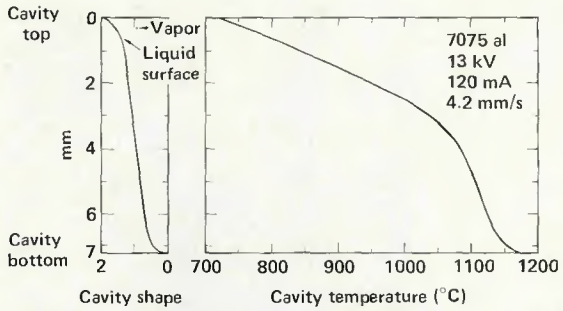

Fig. 8—Approximated cavity shape during welding and typical measured cavity temperature profile for 7075 aluminum

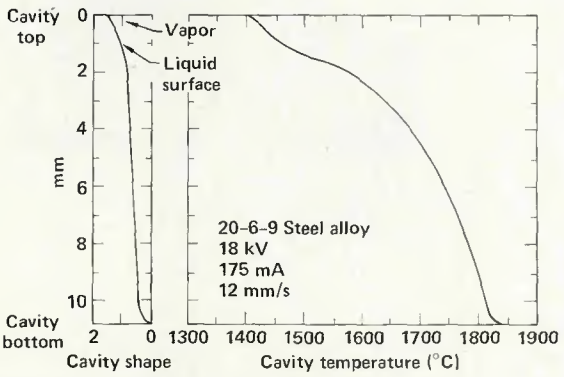

Fig. 9—Approximated cavity shape during welding and typical measured cavity profile for 20-6-9 steel alloy

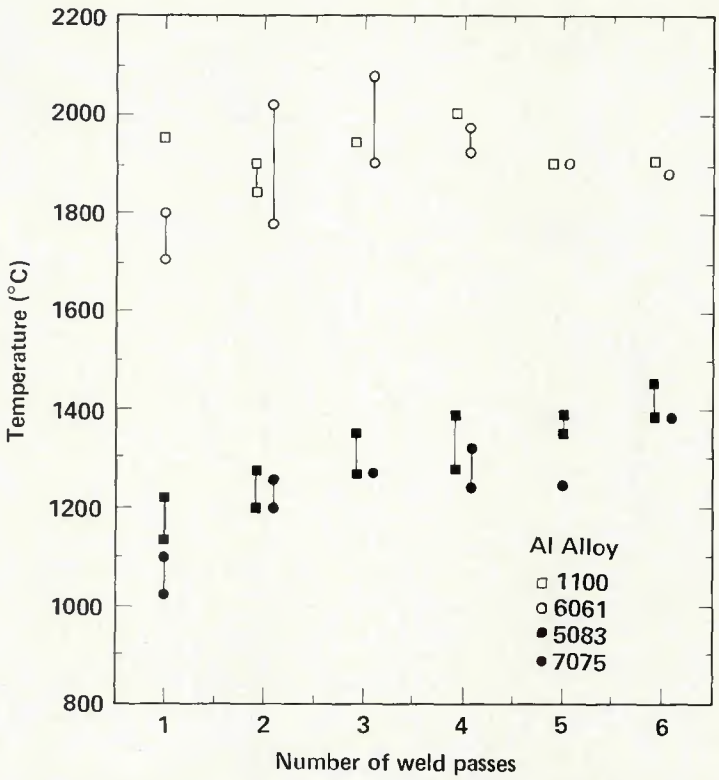

Fig. 10—Variation of peak measured temperature with number of weld passes

vapor was in equilibrium with the liquid. Considering a quasi-steady cavity a force balance on the surface of the molten metal at the bottom shows that the pressure of the metal vapor, p_v, required to maintain equilibrium with the surface tension and hydrostatic head forces is by:[7]

$$P_v = 2\sigma/r + \rho gh \qquad (5)$$

Here σ is the surface tension, r the radius of curvature of the molten metal at the cavity base, ρ the metal density and h the cavity depth. For typical weld cavities the hydrostatic head term ρgh, is found to be small compared to the surface tension effect (on the order of 10%).

A first approximation to the vapor pressure can be obtained by estimating the cavity base radius from a postweld section if the surface tension of the metal is known. Data for the latter as a function of temperature are available for pure metals.[10] Fortunately, surface tension variation with temperature is modest compared to vapor pressure. Hence it is anticipated that reasonably accurate values of σ in equation (5) will yield acceptable values for p_v. From the calculated values of p_v the associated temperature can be determined using vapor pressure data for pure metals.[11]

The above procedure was carried out for pure aluminum and for steel (using values of σ for iron). Assuming a cavity base radius of 0.05 cm and apparent emissivity of 0.3 for Al-1100 predicted peak temperatures were about 5% higher than measured. With the same cavity base radius and an apparent emissivity of 0.6, predicted values for steel agreed within ±5% of measured values.

These variations are within the accuracy of the measurements and tend to confirm the concept that vapor pressure plays a major role in supporting EB weld cavities and that close to thermal equilibrium conditions exist in the cavity. Application of this approach to alloys with highly volatile components is being studied. It will be necessary to develop a procedure for determining the appropriate values of surface tension and vapor pressure.

Table 3—Microanalysis[a] of Aluminum Alloys by wt-% After Six Weld Passes

Alloy	and location	Zn	Mn	Mg	Cu
5083	Base metal	—	0.83	3.74	—
	Weld region	—	0.63	3.47	—
6061	Base metal	0.12	—	0.78	—
	Weld region	0.02	—	0.65	—
7075	Base metal	6.1	—	2.1	1.3
	Weld region	4.9	—	2.0	1.3

[a] 2 to 4% relative error.

Conclusions

1. EB welding cavity base surface temperatures are relatively constant with varying penetration depth for a specific material.

2. Comparison of temperature recordings with weld root sections indicated no correlation between spiking conditions and measured temperature level.

3. The peak cavity surface temperatures for Al-6061, Al-2024, Al-5083 and Al-7075 are lower than that of Al-1100 because they each contain significant amounts of highly volatile magnesium and zinc.

4. Temperature measurements of the cavity base after repeated weld passes indicate that, when very small amounts of highly volatile elements are evaporated, there is a substantial increase in temperature; this explains why the amount of volatile elements in an alloy can have a dramatic effect on the behavior of the cavity during welding.

Acknowledgment

The work discussed in this paper was performed under the auspices of

the U. S. Department of Energy by the Lawrence Livermore Laboratory under contract number W-7045-ENG-48.

References

1. Tong, H., and Giedt, W. H., "Depth of Penetration During Electron Beam Welding," *Journal of Heat Transfer,* Trans. ASME, Ser. C. Vol. 93, (2), 1971.

2. Schauer, D. A., "Thermal and Dynamic Effects in Electron Beam Welding Cavities," Ph.D. Thesis, University of Calif., Dept. of Mechanical Engineering, Davis, Calif., 1977.

3. Shintaku, S. M., "Temperature Distributions in Electron-Beam Welding Cavities," M.S. Thesis, University of California, Dept. of Mechanical Engineering, Davis, California, 1976.

4. Siegel, R., and Howell, J. R., *Thermal Radiation Heat Transfer,* McGraw-Hill, New York, 1972, pp. 111-113.

5. Sparrow, E. M., and Cess, R. D., *Radiation Heat Transfer,* Brooks/Cole Publishing Co., Belmont, California, 1966.

6. Sadykov, B. S., "Temperature Dependence of the Radiation Power of Metals," *High Temperature,* Vol. 3, (3), 1965, pp. 389-394.

7. Touloukain, Y. S. (Ed.), *Thermophysical Properties of High Temperature Solid Materials,* MacMillan Co., New York, 1967.

8. Lin, S. H., and Sparrow, E. M., "Radiant Interchange Among Curved Specularly Reflecting Surfaces—Application to Cylindrical and Conical Cavities," *J. of Heat Transfer,* C 87, 1965, pp. 299-307.

9. Ol'Shanskii, N. A., *et al.,* "The Electron-Beam Welding of Thick Metals Using Low Voltage Beams," *Automatic Welding,* Vol. 25, (11), 1972.

10. Wilson, J. R., "The Structure of Liquid Metals and Alloys," *Metallurgical Reviews,* Vol. 10, (40), 1965.

11. Honig, R. E., "Vapor Pressure Data for the Solid and Liquid Elements," *RCA Review,* Vol. 23, December 1962, pp. 567-586.